

# CHARACTERIZATION OF ONE-DIMENSIONAL TEXTURE --- A POINT PROCESS APPROACH

*M. Zacksenhouse, G. Abramovich, and G. Hetsroni*

Faculty of Mechanical Engineering  
Technion, Israel Institute of Technology  
Haifa 32000, Israel

## ABSTRACT

The distance between 'texture primitives' is of major interest in characterizing texture images. This is especially natural when the texture primitives are elongated structures aligned in parallel to a common main axis, and the distance is measured along the perpendicular axis. Such images arise, for example, in flow visualization studies, where the elongated structures are low-speed streaks. A point process based texture generation model is developed for the one-dimensional texture along lines perpendicular to the streaks. The point process models the location of the edges of the streaks, and using edge detection techniques, its probability density function (pdf) can be estimated by the histogram of the distances between the edges. It is shown that for the studied images the resulting histogram is wide (coefficient of variation larger than half), and demonstrated that in this case, previously suggested auto-correlation based methods are not adequate.

## 1. INTRODUCTION

Texture images may be described by simple texture primitives that are arranged in the image according to some rule, which may be periodic or quasi-periodic, statistical, or semantic. Spectral, statistical and structural approaches to texture analysis have been developed to address these different cases [6]. However, while the spectral and structural approaches characterize the distribution of the texture primitives, the statistical approach characterizes only the resulting distribution of gray levels. Thus, when the texture primitives are arranged stochastically the relevant statistical methods do not provide direct characterization of the distance between the texture primitives.

A special subset of texture images of interest here, is based on elongated texture primitives placed in parallel to each other (Figure 1). In this case the two-dimensional texture image is being reduced to a one-dimensional texture along image lines perpendicular to the major axis of the elongated primitives (along columns of the image in Figure 1). The position of the elongated texture primitives along that direction may be specified by a one-dimension point process. We have developed a point process based texture line generation model and used it to propose image processing algorithm to characterize the point process model and analysis tools to evaluate the shortcoming of spectral approaches in characterizing such images.

The images studied here are taken by infra-red camera using a new technique for visualizing the structure of turbulent flow near the wall. The overall goal of the research is to study the

factors affecting heat transfer at the wall---a process of tremendous economic consequences. Previous visualization studies [8] have demonstrated the existence of coherent structures in the turbulent boundary layer. The coherent structures next to the wall are high speed regions and low speed streaks (the dark and light bands in the image of Figure 1). Important parameters concerning the coherent structures include the distance and extent of the low velocity streaks.

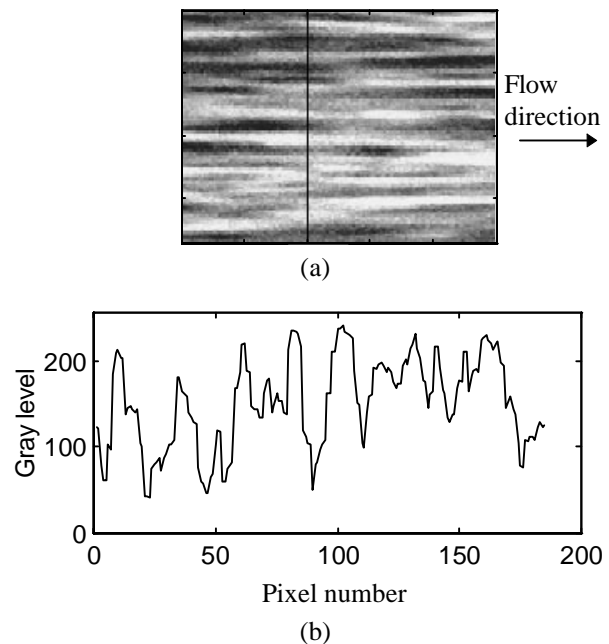


**Figure 1.** (a) Thermal image (185 by 250 pixels) showing low-velocity high temperature streaks (bright structures) separated by high-velocity low-temperature dark regions. (b) A cross section of the image along the indicated column.

### 1.1 Previous Approaches

Previous analysis algorithms, using different visualization techniques, were based on spatial correlation of arrays of measurements taken perpendicular to the flow (such as columns in the image of Figure 1). The distance between the streaks was estimated, for example, by the distance between zero-crossing in the correlation signal. However, the averaged correlation exhibited very flat peaks [5[1], as demonstrated in Figure 2 for the current study, making such estimations unreliable.

In an effort to overcome this problem, it has been proposed [1] to locate the first positive peak of the auto-correlation of individual measurement arrays and use the average lag of the first peak as an estimate of the distance between the streaks. However, this method is questionable, given the flat nature of the averaged auto-correlation, as will be discussed later.

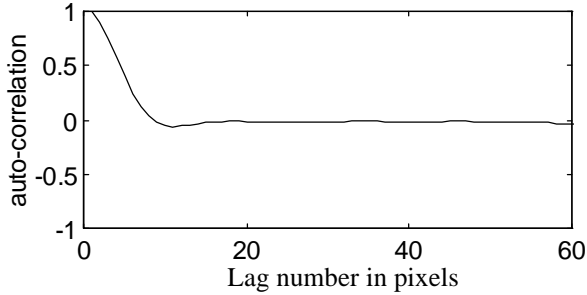


**Figure 2.** Auto-correlation of columns of thermal images averaged over 78 columns one from each image in a sequence of 78 images taken 0.5sec apart.

## 1.2 Visualization Technique

The visualization technique and experimental setup are described in [7]. Shortly, an infra-red camera is used to measure the temperature field on the surface of a heater made of 50  $\mu\text{m}$  constantan foil, which was installed in the floor of the duct. It is assumed that the heater is thin enough so that the temperature measured on the outside reflects well the temperature of the heater exposed to the flow. Hence, the velocity field of the flow, which affects the local heat transfer, is visualized by imaging the temperature field (Figure 1). Low temperature (dark regions) reflects high-speed and high temperatures (light region) reflects low speed. The temperature range of  $2^\circ\text{C}$  is imaged into 256 gray levels. The image of Figure 1 includes 185 by 250 pixels and covers an area of 13.3 by 10.4 cm.

## 2. TEXTURE GENERATION MODEL

### 2.1 Point Process based model

Given the elongated texture of the flow images, we are interested in characterizing the width and distance between the streaks in the direction perpendicular to the flow. While the temperature may vary from one streak to another and across a streak, we neglect this information in this stage and retain only the information relating to the position of each streak and its width. This information is best represented by the edges of the streaks.

Along lines perpendicular to the flow, the edges appear as sets of points marking the beginning and end of the streaks. From an information point of view, the location of these points can be modeled as a stochastic point process on the line [3]. Since two types of points are generated, those indicating the beginning and end of the streak, a marked point process is used, where the mark associated with each point is either '-' (beginning) or '+' (end) of a streak. Clearly, the marks are alternating as each

'beginning of streak' should be associated with an 'end-of-streak'. Thus the underlying marked point process can be described by the statistics of the intervals between '+' points to '-' points and '-' points to '+' points.

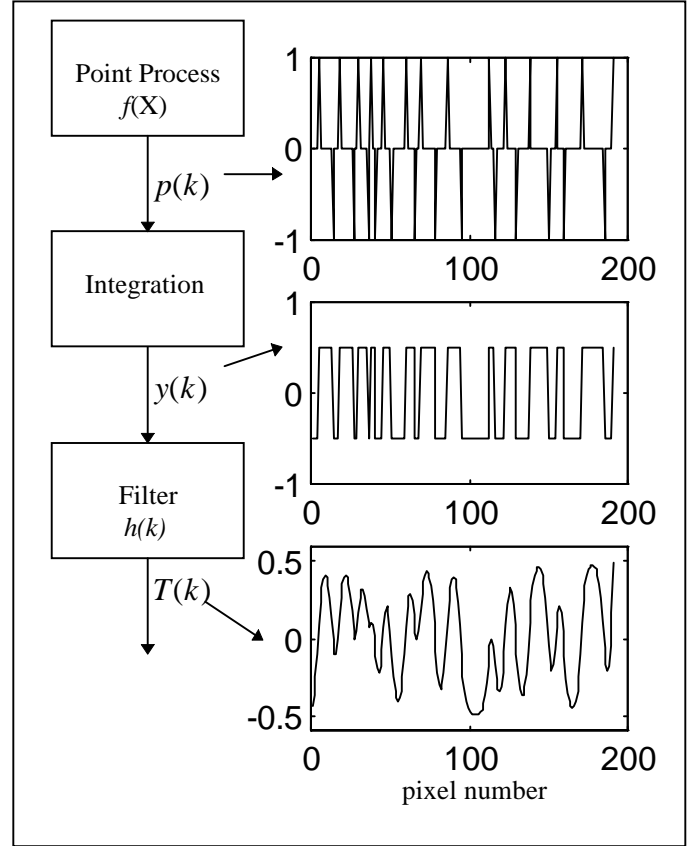


**Figure 3.** Point process based line texture generation model

While not critical for the development of the model, we assume here that the statistics of the intervals between the points is the same regardless of their mark. We denote by  $f(X)$  the probability density function (pdf) of the intervals between the points. A realization of a point process is a set of intervals  $\{X_i\}$  between the points. Since points can have either a '+' or a '-' mark, each realization can be described by a bipolar pulse train  $p(k)$ , taking the value +1 or -1 when a point with mark '+' or '-' exists in the interval  $[k\delta, (k+1)\delta]$ , respectively, and 0 otherwise ( $\delta$  is the spatial resolution of a pixel). Thus, the measured temperature profile along an image column  $T(k)$  can be modeled as the output of a low pass filter whose input is a 'box' signal generated by summing the pulse train:

$$y(k) = \sum_{l=1}^{l=k} p(l) \quad \text{with } y(0) = -.5$$

Assuming that the first point is marked '+' and that there is an even number of points, the resulting signal  $y(k)$  takes the values +.5 or -.5 and is centered around zero. Finally,

$$T(k) = y(k) \otimes h(k)$$

where,  $h(k)$  is the impulse response of the spatial filter and  $\otimes$  denotes convolution. The stochastic texture line generation model is shown in Figure 3.

## 2.2 Auto-correlation Analysis

From the stochastic texture generation model of Figure 3, the auto-correlation of the output signal  $A_T(m)$  can be evaluated based on the probability density function  $f(X)$  of the underlying point process model. First, the auto-correlation  $A_p(m)$  of the pulse train is the discrete version of the continuous space auto-correlation:

$$A_p(m) = \int_{\alpha=0}^{\delta} \int_{\beta=-\alpha}^{\delta-\alpha} A_c(m\delta + \beta) d\beta d\alpha$$

where the continuous space auto-correlation  $A_c$  is given as the sum of the  $r$ -fold convolution  $f_{(r)}(X)$  of the pdf [3]:

$$\begin{aligned} A_c(X) &= \sum_{r=1}^{\infty} (-1)^r f_{(r)}(X) & X > 0 \\ &= A_c(-X) & X < 0 \\ &= 1 & X = 0 \end{aligned}$$

The auto-correlation of the ‘box’ signal  $y(k)$  generated by summing the pulse train  $p(k)$ , is given by:

$$A_y(m) = \sum_{n=m}^{\infty} \sum_{l=-\infty}^n A_p(l)$$

The final output signal is a filtered version of the box signal and its auto-correlation is given by [9].

$$A_T(m) = A_y(m) \otimes h(m)$$

Thus, the auto-correlation of the output signal is an integrated and filtered version of the auto-correlation of the underlying point process model.

## 2.3 Simulation

The texture generation model has been simulated to demonstrate the relationship between the auto-correlation of the signals at its different stages. Gamma pdf [3], shifted by a single pixel, were used to produce either a narrow pdf with coefficient of variation (CV) less than half or a wide pdf with CV greater than half, respectively (Table I). A narrow pdf resulted in an oscillating average auto-correlation at all the stages of the model (Figure 4, upper panel) and the location of the first peak, or alternatively the location of the peak in the power spectrum (not shown), provides a reliable estimate of the mean interval  $\mu$ . In contrast, a wide pdf resulted in an average auto-correlation that exhibits weak oscillations which are smeared by the integration and the filtering stages (Figure 4, lower panel). In this case, neither the

peaks of the auto-correlation nor those in the power spectrum provide reliable estimates of the mean interval  $\mu$ .

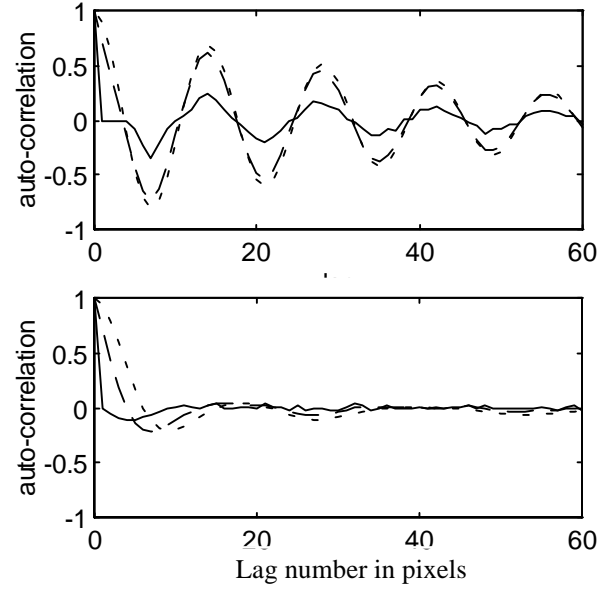


Figure 4. Average auto-correlation of simulated pulse train (solid), box train (dashed) and output signal (dots) at the different stages of the texture generation model based on a narrow pdf (upper) and a wide pdf (lower) with parameters of Table I. Average based on 16 samples of 185 long vectors.

Considering a single column, the auto-correlation of the output signal does exhibit a first peak. However, the integration and filtering stages have the effect of shifting the first positive peak toward higher lags. Simulations results, with the wide pdf of Table I, demonstrate that the estimator proposed in [1], based on the average lag of the first peak in the auto-correlation of individual columns, is biased by as much as 40%.

## 3. FEATURE EXTRACTION METHOD

### 3.1 Edge Detection

The texture generation model is based on a point process model to produce the location of the edges of the streaks along lines perpendicular to the flow. Thus, samples of the underlying point process model can be recovered from the images by detecting the edges of the streaks. We have used a Canny-based edge detection method [2] and applied specially designed Dilation and Erosion morphological operators for linking edges in the direction of the flow (row-wise). The detected edges and thus the measured distances are sensitive to the threshold used in the edge detection algorithm. However, the sensitivity is modest along a wide range of threshold values and we selected the threshold at the upper limit of this range. The edge detection output is demonstrated in Figure 5, overlaid on top of the processed image.

The gradient operator applied in edge detection has a pre-whitening effect, as suggested previously [4]. However, there

the resulting image was used to generate a histogram of the decorrelated gray levels, while here the edges are localized and the histogram of the distance between the edges is computed.

### 3.2 Distance and Width of Streaks

Given the highly correlated nature of the images (in the direction of the flow), only a single column from each image has been considered as an independent sample of the underlying point process model. Different samples were selected from seventy-eighth images taken 0.5sec apart to avoid temporal correlation. Since the edge detection procedure is not perfect, candidate columns were tested for validity before being considered as samples of the underlying point process. Valid columns should have included alternating '+' and '-' edges.

The histograms of the distances (normalized to unit area), and the best matching shifted Gamma distributions, are shown in Figure 5; the corresponding parameters, are given in Table I. The results indicate that the underlying point process model is indeed wide.



(a)

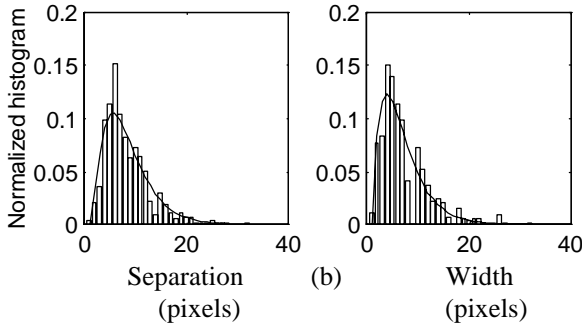


Figure 5. Detected edges overlaid on thermal image (a). Normalized histograms (b) of distance between edges bounding the dark regions (separation between streaks), and between edges bounding bright regions (width of streaks), with best matching shifted Gamma distribution parameterized in Table I.

## 4. SUMMARY

We have found that the separation between the streaks and the width of the streaks are widely distributed. In the framework of the texture generation model proposed here, this information characterizes the underlying point process model. We have shown that when the pdf of the underlying point process model is as wide as the resulting histograms, auto-correlation based methods do not provide a reliable technique for estimating the mean distance between the streaks. The edge-based method proposed here provides a full characterization of the separation and width of the streaks; not only their mean value. Further analysis using this technique can be applied to study how the separation between the streaks, and how the temperature of the streaks, depend on the width of the streak.

Case	Parameters			Gamma		
	mean $\mu$	$\sigma$	min	$\rho$	$\alpha$	s
<b>Simulation</b>						
Narrow (a)	7	1	1	6	36	1
Wide (b)	7	4	1	0.375	2.25	1
<b>Data</b>						
Width	7.3	4.3	1	0.34	2.15	1
Separation	8.4	4.6	1	0.36	2.65	1

Table I Parameters of pdf used in simulations and of histograms derived from data analysis; along with coefficients of the best matching shifted Gamma pdf.

$$f(X) = \rho(\rho(X - s))^{\alpha-1} e^{-\rho(X-s)} / \Gamma(\alpha)$$

## 5. REFERENCES

- [1] Achia and Thompson D.W. "Structure of the Turbulent Boundary in Drag-reducing Pipe Flow". *J. Fluid Mech.* **81**, 439-464, 1977.
- [2] Canny J. "A Computational Approach to Edge Detection", *IEEE Trans. PAMI*, **8**(6), 1986.
- [3] Cox D.R., *Renewal Theory*, John Wiley & Sons, Inc, 1962.
- [4] Faugeras O.D., Pratt W.K., "Decorrelation Methods of Texture Feature Extraction". *IEEE Trans. PAMI*, **2**(4), 1980.
- [5] Fortuna, G. and Hanratty, T.J. "The influence of drug-reducing polymers on turbulence in viscous sub-layer" *J Fluid Mech*, **53**, 575-586, 1972.
- [6] Gonzalez R.C. and Wintz P. *Digital Image Processing* Addison-Wesley Publishing Company, 1987.
- [7] Hetsroni G. and R. Rozenblit "Heat Transfer to liquid-solid mixture in a flume" *Int. J. Multiphase Flow* **20**, 671-689, 1994..
- [8] Kline S.J., Reynolds W.C., Schraub F.A. and Rundstadler P.W. "The Structure of Turbulent Boundary Layer". *J. Fluid Mech*, **30**, 741-773, 1967.
- [9] Papoulis A. *Probability, Random Variables and Stochastic Processes*. McGraw-Hill 1985